UNCLASSIFIED

AD **404 167**

Reproduced
by the

DEFENSE DOCUMENTATION CENTER

FOR

SCIENTIFIC AND TECHNICAL INFORMATION

CAMERON STATION, ALEXANDRIA, VIRGINIA

UNCLASSIFIED

63-3-4

AFCRL-63-66
March 1963

USCEC Report 82-210
EE-20

UNIVERSITY OF SOUTHERN CALIFORNIA

SCHOOL OF ENGINEERING

RADIATION FROM AN AXIALLY SLOTTED CYLINDER WITH A RADIALLY INHOMOGENEOUS PLASMA COATING

W. V. T. Rusch

MAY 21 1963

TISIA A
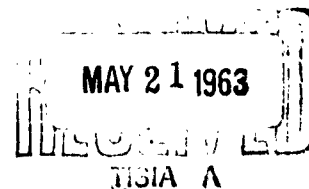
ELECTRICAL ENGINEERING DEPARTMENT

Engineering

⑥ RADIATION FROM AN AXIALLY SLOTTED CYLINDER WITH A RADIALLY INHOMOGENEOUS PLASMA COATING,

ELECTRICAL ENGINEERING DEPARTMENT
UNIVERSITY OF SOUTHERN CALIFORNIA
LOS ANGELES 7, CALIFORNIA

Prepared
for

ABSTRACT

Radiation patterns ~~have been~~ WERE computed for an axial slot on an infinite circular cylinder coated with a radially inhomogeneous plasma sheath. The relative dielectric constant was assumed to have three types of radial dependence: monotonic with a minimum at the inner edge of the sheath but with no portion of the sheath below plasma resonance; monotonic with the inner portion of the sheath below plasma resonance; parabolic with a minimum within the sheath and the inner portion of the sheath below resonance. The radial wave functions within the sheath are obtained in the form of infinite series. The resulting radiation patterns are found to be sharply directed in the forward direction relative to the equivalent free-space pattern. These sharply forward-directed patterns are consistent with the interpretation of a diffusion-type process within layers of the sheath below cutoff and a predominantly refraction-type process within layers above cutoff.

TABLE OF CONTENTS

LIST OF ILLUSTRATIONS

I. INTRODUCTION

The recent literature contains numerous analyses of radiation from slot antennas on dielectric-clad and plasma-clad cylinders. These analyses are especially useful in predicting the requirements for communicating with high-speed, re-entry vehicles of cylindrical shape. With few exceptions the sheath has been represented by a homogeneous coating with an equivalent dielectric constant, determined by the "average" properties of the sheath. It is to be expected, however, that important effects caused by density gradients which exist in re-entry sheaths will seriously modify the radiation characteristics of the homogeneous model.

Consequently a study of the radiation pattern of a slotted cylinder clad with a radially inhomogeneous sheath has been undertaken. The assumed radial variation of the dielectric constant is highly idealized (parabolic), yet it corresponds closely to sheath conditions of considerable physical interest. It can be shown that the equivalent dielectric constant of a cold plasma is approximately:

$$\frac{\epsilon}{\epsilon_0} = 1 - \frac{Ne^2}{m \, \epsilon_0 \, \omega^2}$$

where N is the electron density. Estimates of the radial distribution of electron density in the plasma sheath surrounding a hypersonic re-entry vehicle indicate a maximum density at or near the surface of the vehicle, and a monotonically decreasing density with increasing distance from the

maximum (Ref. 1). Such a negative gradient of electron density would cause the dielectric constant to increase with increasing radius from a value less than unity to the free-space value. Furthermore, it may not be unreasonable to assume that over a range of radii the electron density is sufficiently large that below certain frequencies the dielectric constant is negative and that region is opaque to propagating waves. By appropriate choice of parameters the radial variation of dielectric constant assumed in the following section can be consistent with both relatively steep negative gradients of electron density and portions of the sheath below cutoff.

The equivalent dielectric constant used in the following analyses is derived with the restriction that nonlinear effects, thermal effects, and the effects of collisions may be neglected. It has been pointed out by Samaddar in the analysis of a similar problem (Ref. 2) and by others (Refs. 3 and 4) that this approximation is no longer valid if the dielectric constant becomes vanishingly small; under such conditions it becomes necessary to use the kinetic theory of plasma behavior. Although several of the numerical examples considered allow the dielectric constant to pass through zero at some radius within the sheath, kinetic theory has not been applied. Consequently the interpretation of some of the curves is limited by the possibility that nonlinear and thermal effects in the vicinity of vanishing dielectric constant may modify the patterns.

II. FORMULATION OF THE PROBLEM

An infinite, perfectly conducting circular cylinder of radius a is coaxial with the z-axis (Fig. 1). The cylinder is covered by an inhomogeneous, isotropic plasma coating of permittivity $\epsilon(k\rho) = \epsilon_0\left[1 - \dfrac{N(k\rho)e^2}{m\epsilon_0\omega^2}\right]$ and permeability μ_0 extending from $a \leq \rho \leq b$. $N(k\rho)$ is the electron density, a function of radius. An infinite axial slot on the surface of the cylinder ($\rho = a$) extends from $-\dfrac{\Delta}{2} \leq \phi \leq +\dfrac{\Delta}{2}$. Because of the assumed nature of the fields in the slot, the tangential electric fields at $\rho = a$ are:

$$E_z(a,\phi) = 0 \tag{1}$$

$$E_\phi(a,\phi) = \begin{cases} 0, \ |\phi| \geq \dfrac{\Delta}{2} & \text{(2a)} \\[3mm] \dfrac{V_0}{a\Delta}, \ |\phi| \leq \dfrac{\Delta}{2} & \text{(2b)} \end{cases}$$

Within the plasma coating from $a \leq \rho \leq b$, the permittivity is assumed to have the following dependence on radius:

$$\epsilon(\rho) = \epsilon_0 f(k\rho) \tag{3}$$

where

$$f(k\rho) = H(k\rho - kc)(k\rho - kc_A) = H(k\rho - kc)^2 + H(k\rho - kc)(kc - kc_A) \tag{4}$$

Consequently $f(k\rho)$, the relative dielectric constant, has three types of radial dependence: monotonic with a minimum at $\rho = a$ but with no portion of the sheath below plasma resonance (Fig. 2a); monotonic with the inner

portion of the sheath below plasma resonance (Fig. 2b); parabolic with a minimum at $\rho_0 > a$ and the inner portion of the sheath below plasma resonance (Fig. 2c). In each case the outer edge of the sheath is defined by $\epsilon(b) = \epsilon_0$.

The corresponding radial variations of electron density are also indicated in Figs. 2a, 2b and 2c.
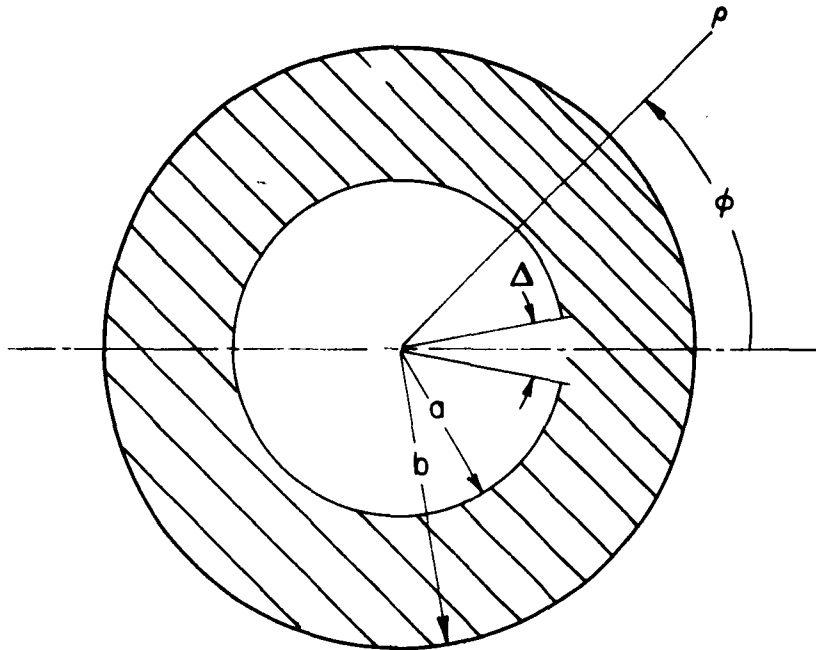
Fig. 1   Cross Section Of Infinite Slotted
Cylinder With Plasma Sheath.

a. Parabolic Monotonic

b. Parabolic Monotonic
   With Cutoff

c. Parabolic Minimum
   With Cutoff
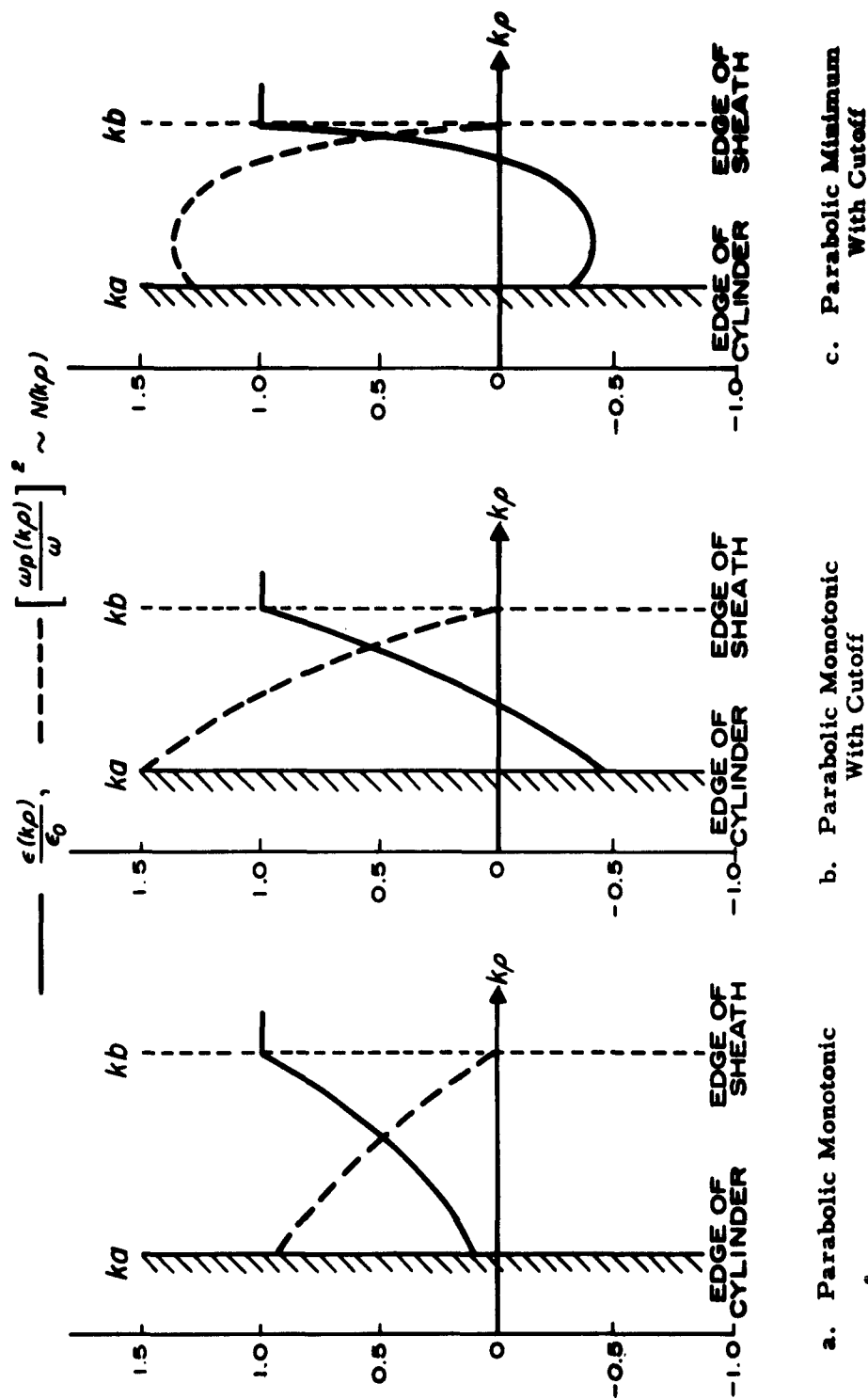
Fig. 2 Three Types Of Radial Dependence Of Dielectric Constant And Electron Density.

III. SOLUTION OF MAXWELL'S EQUATIONS

IN THE INHOMOGENEOUS MEDIUM

For an assumed harmonic time dependence $e^{-i\omega t}$ (suppressed throughout), Maxwell's equations become:

$$\nabla \times \bar{H} = \frac{\partial \bar{D}}{\partial t} = -i\omega \epsilon(\rho) \bar{E} \tag{5a}$$

$$\nabla \times \bar{E} = -\frac{\partial \bar{B}}{\partial t} = +i\omega \mu_0 \bar{H} \tag{5b}$$

The electric field may be eliminated, yielding

$$\nabla \times \nabla \times \bar{H} = \left[\frac{\nabla \epsilon(\rho)}{\epsilon(\rho)}\right] \times (\nabla \times \bar{H}) + \omega^2 \mu_0 \epsilon_0 f(k\rho) \bar{H} \tag{6}$$

Since no radial component of the magnetic intensity will be excited, it is expected that $\bar{H}$ can be expressed as the curl of a radially directed vector function of ρ and ϕ (after the vector wave-function method of Stratton and Hansen [Refs. 5 and 6]):

$$\bar{H} = \nabla \times \left\{ (k\rho) R(k\rho) H(\phi) \bar{a}_\rho \right\} \tag{7}$$

Substitution of this quantity into Eq. 6 yields

$$\frac{\partial}{\partial \phi}\left\{ \frac{k}{\rho^2} R(k\rho) H''(\phi) + \frac{H(\phi)}{\rho} \frac{\partial}{\partial \rho}\left[k\rho \frac{\partial R(k\rho)}{\partial \rho}\right] - \frac{kH(\phi)}{f(k\rho)} \frac{\partial f(k\rho)}{\partial \rho} \frac{\partial R(k\rho)}{\partial \rho} + \omega^2 \mu_0 \epsilon_0 f(k\rho) k R(k\rho) H(\phi) \right\} \bar{a}_z = 0 \tag{8}$$

Equation 8 is satisfied by requiring the bracketed quantity itself to be

zero. This condition then yields the two equations defining $R(k\rho)$ and $H(\phi)$:

$$H''(\phi) + m^2 H(\phi) = 0 \tag{9}$$

$$\left\{(k\rho)^2\right\} R''(k\rho) + \frac{(k\rho)}{f(k\rho)} \left\{f(k\rho) - (k\rho)\frac{df(k\rho)}{d(k\rho)}\right\} R'(k\rho) + \left\{(k\rho)^2 f(k\rho) - m^2\right\} R(k\rho) = 0 \tag{10}$$

The solutions of Eq. 9 are clearly

$$H(\phi) = C_m \cos m\phi + D_m \sin m\phi \tag{11}$$

The solutions of Eq. 10 are two independent radial functions which will be determined in a later section:

$$R(k\rho) = A_m R_m^{(1)}(k\rho) + B_m R_m^{(2)}(k\rho) \tag{12}$$

In free space $f(k\rho) = 1$ and Eq. 10 becomes Bessel's equation

$$(k\rho)^2 R''(k\rho) + (k\rho) R'(k\rho) + \left[(k\rho)^2 - m^2\right] R(k\rho) = 0 \tag{10a}$$

In this special case $R_m^{(1)}(k\rho)$ and $R_m^{(2)}(k\rho)$ are the standard Bessel or Hankel functions of integral order.

IV. MATCHING THE BOUNDARY CONDITIONS

For the geometry of the plasma-clad axially slotted cylinder described previously, the fields may be expanded in the following manner:

$$E_{\emptyset}(\rho,\emptyset) = \frac{ik}{\omega\epsilon(\rho)} \sum_{m=0}^{\infty} \frac{d}{d\rho}\left[A_m R_m^{(1)}(k\rho) + B_m R_m^{(2)}(k\rho)\right]\cos m\emptyset \qquad (13a)$$

$$H_z(\rho,\emptyset) = -k \sum_{m=0}^{\infty}\left[A_m R_m^{(1)}(k\rho) + B_m R_m^{(2)}(k\rho)\right]\cos m\emptyset \qquad (13b)$$

$a \le \rho \le b$

$$E_{\emptyset}(\rho,\emptyset) = \frac{ik}{\omega\epsilon_0} \sum_{m=0}^{\infty} \frac{d}{d\rho}\left[C_m H_m^{(1)}(k\rho)\right]\cos m\emptyset \qquad (14a)$$

$$H_z(\rho,\emptyset) = -k \sum_{m=0}^{\infty} C_m H_m^{(1)}(k\rho)\cos m\emptyset \qquad (14b)$$

$\rho \ge b$

Matching the boundary conditions on the tangential field at $\rho = a$ and $\rho = b$ and letting $\Delta \to 0$, it can be shown that

$$C_m = \frac{-i\, G_0\, f_{m1}\left[f_{m2} - if_{m3}\right]}{(1+\delta_{0m})\left[(f_{m2})^2 + (f_{m3})^2\right]} \quad \text{where} \quad G_0 = \frac{\omega\,\epsilon(a)\,V_0}{\pi a k^2} \qquad (15)$$

and

$$f_{m1} = R_m^{(1)'}(kb)\, R_m^{(2)}(kb) - R_m^{(2)'}(kb)\, R_m^{(1)}(kb) \qquad (16)$$

$$f_{m2} = R_m^{(1)'}(ka)\left\{J_m(kb)\left[\frac{m}{kb} R_m^{(2)}(kb) - R_m^{(2)'}(kb)\right] - J_{m+1}(kb) R_m^{(2)}(kb)\right\}$$

$$- R_m^{(2)'}(ka)\left\{J_m(kb)\left[\frac{m}{kb} R_m^{(1)}(kb) - R_m^{(1)'}(kb)\right] - J_{m+1}(kb) R_m^{(1)}(kb)\right\} \qquad (17a)$$

$$f_{m3} = R_m^{(1)'}(ka)\left\{N_m(kb)\left[\frac{m}{kb} R_m^{(2)}(kb) - R_m^{(2)'}(kb)\right] - N_{m+1}(kb) R_m^{(2)}(kb)\right\}$$

$$- R_m^{(2)'}(ka)\left\{N_m(kb)\left[\frac{m}{kb} R_m^{(1)}(kb) - R_m^{(1)'}(kb)\right] - N_{m+1}(kb) R_m^{(1)}(kb)\right\} \qquad (17b)$$

Upon substitution of Eq. 15 and the asymptotic value of the Hankel function into Eq. 14b, the far-zone field becomes:

$$H_z(k\rho) \xrightarrow[k\rho \longrightarrow \infty]{} -G_0\left(\frac{2k}{\pi\rho}\right)^{1/2} e^{i\left(k\rho - \frac{3\pi}{4}\right)} \sum_{m=0}^{\infty} \frac{e^{-i\frac{m\pi}{2}} f_{m1}(f_{m2} - if_{m3})}{(1+\delta_{0m})\left[(f_{m2})^2 + (f_{m3})^2\right]} \cos m\phi$$

(18)

V. SOLUTION FOR THE RADIAL FUNCTIONS

Inspection of Eq. 10 reveals that $\rho = c$ is a regular point of the differential equation. It is then to be expected that $R_m^{(1)}(k\rho)$ and $R_m^{(2)}(k\rho)$ can be expanded as an infinite power series about $\rho = c$ (Ref. 7). Equation 10 can then be rewritten:

$$A(k\rho) R''(k\rho) + B(k\rho) R'(k\rho) + C(k\rho) R(k\rho) = 0 \qquad (19)$$

where

$$A(k\rho) = \sum_{n=1}^{4} a_n (k\rho - kc)^n \qquad (20)$$

$$a_1 = H(kc)^2 (kc - kc_A) \qquad (20a)$$

$$a_2 = H(kc)(3kc - 2kc_A) \qquad (20b)$$

$$a_3 = H(3kc - kc_A) \qquad (20c)$$

$$a_4 = H \qquad (20d)$$

-9-

and

$$B(k\rho) = \sum_{n=0}^{3} b_n(k\rho - kc)^n \tag{21}$$

$$b_0 = -H(kc)^2(kc - kc_A) = -a_1 \tag{21a}$$

$$b_1 = -H(kc)(3kc - kc_A) \tag{21b}$$

$$b_2 = -3H(kc) \tag{21c}$$

$$b_3 = -H = -a_4 \tag{21d}$$

and

$$C(k\rho) = \sum_{n=1}^{6} c_n(k\rho - kc)^n \tag{22}$$

$$c_1 = -m^2 H(kc - kc_A) \tag{22a}$$

$$c_2 = H\left[H(kc)^2(kc - kc_A)^2 - m^2\right] \tag{22b}$$

$$c_3 = 2H^2(kc)(2kc - kc_A)(kc - kc_A) \tag{22c}$$

$$c_4 = H^2\left[6(kc)^2 - 6(kc)(kc_A) + (kc_A)^2\right] \tag{22d}$$

$$c_5 = 2H^2(2kc - kc_A) \tag{22e}$$

$$c_6 = H^2 \tag{22f}$$

If $R_m(k\rho)$ is assumed to be of the form

$$R_m(k\rho) = \sum_{n=0}^{\infty} d_n(k\rho - kc)^{n+a} \tag{23}$$

then substitution into Eq. 19 yields the following indicial equation:

$$a\left[a_1(a-1) + b_0\right] = 0 \tag{24}$$

The solutions of Eq. 24 are

$$a = 0 \tag{24a}$$

$$a = 1 - \frac{b_0}{a_1} = 2 \tag{24b}$$

Following the procedure outlined in Ref. 7 if a solution is assumed using the algebraic smaller of the two indices, two independent infinite series are generated if $m = 0$. It can be shown that if $m = 0$:

$$R_0^{(1)}(k\rho) = \sum_{n=0}^{\infty} {_0}d_n^{(1)} (k\rho - kc)^{n+2} \tag{25}$$

where

$${_0}d_0^{(1)} \equiv 1 \tag{25a}$$

$${_0}d_n^{(1)} = -\left\{ (n+1)(na_2 + b_1)_0 d_{n-1}^{(1)} + n\left[(n-1)a_3 + b_2\right]_0 d_{n-2}^{(1)} + \left[(n-1)(n-3)a_4 + c_2\right]_0 d_{n-3}^{(1)} \right.$$

$$\left. + c_3 {_0}d_{n-4}^{(1)} + c_4 {_0}d_{n-5}^{(1)} + c_5 {_0}d_{n-6}^{(1)} + c_6 {_0}d_{n-7}^{(1)} \right\}/(n+2)na_1, \; n \geq 1 \tag{25b}$$

and

$$R_0^{(2)}(k\rho) = \sum_{n=0}^{\infty} {_0}d_n^{(2)} (k\rho - kc)^n \tag{26}$$

where

$${_0}d_0^{(2)} \equiv 1 \tag{26a}$$

$${_0}d_1^{(2)} = 0 \tag{26b}$$

$${_0}d_2^{(2)} = 0 \tag{26c}$$

$$_0 d_n^{(2)} = -\Big\{(n-1)\Big[(n-2)a_2 + b_1\Big]_0 d_{n-1}^{(2)} + (n+2)\Big[(n-3)a_3 + b_2\Big]_0 d_{n-2}^{(2)}$$

$$+ \Big[(n-3)(n-5)a_4 + c_2\Big]_0 d_{n-3}^{(2)} + c_3\,_0 d_{n-4}^{(2)} + c_4\,_0 d_{n-5}^{(2)}$$

$$+ c_5\,_0 d_{n-6}^{(2)} + c_6\,_0 d_{n-7}^{(2)}\Big\}/n(n-2)a_1, \quad n \geq 3 \qquad (26d)$$

In the case $m \neq 0$, both roots of the indicial equation yield the same series:

$$R_m^{(1)}(k\rho) = \sum_{n=0}^{\infty}\,_m d_n^{(1)}(k\rho - kc)^{n+2} \qquad (27)$$

where

$$_m d_0^{(1)} \equiv 1 \qquad (27a)$$

$$_m d_n^{(1)} = -\Big\{(n+1)(n\,a_2 + b_1)\,_m d_{n-1}^{(1)} + \Big[n\big[(n-1)a_3 + b_2\big] + c_1\Big]_m d_{n-2}^{(1)}$$

$$+ \Big[(n-1)(n-3)a_4 + c_2\Big]_m d_{n-3}^{(1)} + c_3\,_m d_{n-4}^{(1)} + c_4\,_m d_{n-5}^{(1)} + c_5\,_m d_{n-6}^{(1)}$$

$$+ c_6\,_m d_{n-7}^{(1)}\Big\}/n(n+2)a_1, \quad n \geq 1 \qquad (27b)$$

$R_0^{(1)}(k\rho)$ is the limiting case of $R_m^{(1)}(k\rho)$ with $m = 0$. A second independent solution can be generated of the form (Ref. 7)

$$R_m^{(2)}(k\rho) = R_m^{(1)}(k\rho)\,\ln(k\rho - kc)^2 + \sum_{n=0}^{\infty}\,_m f_n(k\rho - kc)^n \qquad (28)$$

Substitution of Eq. 28 into Eq. 19 then yields the recursion relations for $_m f_n$:

$$_m f_0 = -\Big\{4a_1/c_1\Big\} \qquad (28a)$$

$$_m f_1 = 0 \tag{28b}$$

$$_m f_2 = 0 \tag{28c}$$

$$
_m f_n = -\left\{ 4(n-1)a_1 {}_m d_{n-2}^{(1)} + 2\left[(2n-3)a_2 + b_1\right] {}_m d_{n-3}^{(1)} + 2\left[(2n-5)a_3 + b_2\right] {}_m d_{n-4}^{(1)} \right.
$$

$$
+ 4(n-4)a_4 {}_m d_{n-5}^{(1)} + (n-1)\left[(n-2)a_2 + b_1\right] {}_m f_{n-1} + \left[(n-2)\left[(n-3)a_3 + b_2\right] + c_1\right] {}_m f_{n-2}
$$

$$
+ \left[(n-3)(n-5)a_4 + c_2\right] {}_m f_{n-3} + c_3 {}_m f_{n-4} + c_4 {}_m f_{n-5} + c_5 {}_m f_{n-6}
$$

$$
\left. + c_6 {}_m f_{n-7} \right\} / n(n-2)a_1, \quad n \geq 3 \tag{28d}
$$

Equations 25, 26, 27, and 28 can then be substituted into Eq. 18 to yield the far-field pattern. Considerable simplification can be accomplished by substitution of the Wronskian relations, developed in Appendix A, into the formulas. The far-field pattern then becomes

$$
P(\phi) = \sqrt{\left[R(\phi)\right]^2 + \left[I(\phi)\right]^2} \tag{29}
$$

where

$$
R(\phi) = \frac{(kc)(kb-kc)(kb-kc_A)}{(kb)(kc-kc_A)} \left\{ \frac{f_{02}}{(f_{02})^2 + (f_{03})^2} + 8(kc)^2 \sum_{m=1}^{\infty} \frac{\left[\cos\frac{m\pi}{2} f_{m2} - \sin\frac{m\pi}{2} f_{m3}\right]}{m^2\left[(f_{m2})^2 + (f_{m3})^2\right]} \cos m\phi \right\} \tag{30}
$$

$$
I(\phi) = \frac{(kc)(kb-kc)(kb-kc_A)}{(kb)(kc-kc_A)} \left\{ \frac{f_{03}}{(f_{02})^2 + (f_{03})^2} + 8(kc)^2 \sum_{m=1}^{\infty} \frac{\left[\sin\frac{m\pi}{2} f_{m2} + \cos\frac{m\pi}{2} f_{m3}\right]}{m^2\left[(f_{m2})^2 + (f_{m3})^2\right]} \cos m\phi \right\} \tag{31}
$$

In the case of a vanishing sheath, i.e., $a = b$, it can easily be shown that Eq. 29 reduces to

$$P(\phi) = \left| \sum_{m=0}^{\infty} \frac{e^{-im\frac{\pi}{2}} \cos m\phi}{(1+\delta_{0m}) H_m^{(1)'}(kb)} \right| \qquad (32)$$

which is the well-known result for a slotted cylinder in free space.

VI. NUMERICAL EVALUATION OF THE FIELDS

The magnitude of the far-zone field pattern (cf. Eq. 18) has been evaluated on a large digital computer for various configurations of dielectric constant. These patterns are plotted in the following figures. An inner sheath radius of $ka = 5$ and an outer radius of $kb = 6$ have been maintained throughout. Only half of each pattern has been plotted since symmetry exists about $\phi = 0$. Each pattern has been normalized to its maximum value (consistently in the forward direction). Consequently, direct amplitude comparisons may not be made between individual patterns. However, comparison of relative pattern shapes has been facilitated by this normalization.

The field patterns plotted in Fig. 3 resulted from a dielectric constant variation of the type indicated in Fig. 2a: a monotonic variation with a minimum at the inner edge of the sheath but with no portion of the
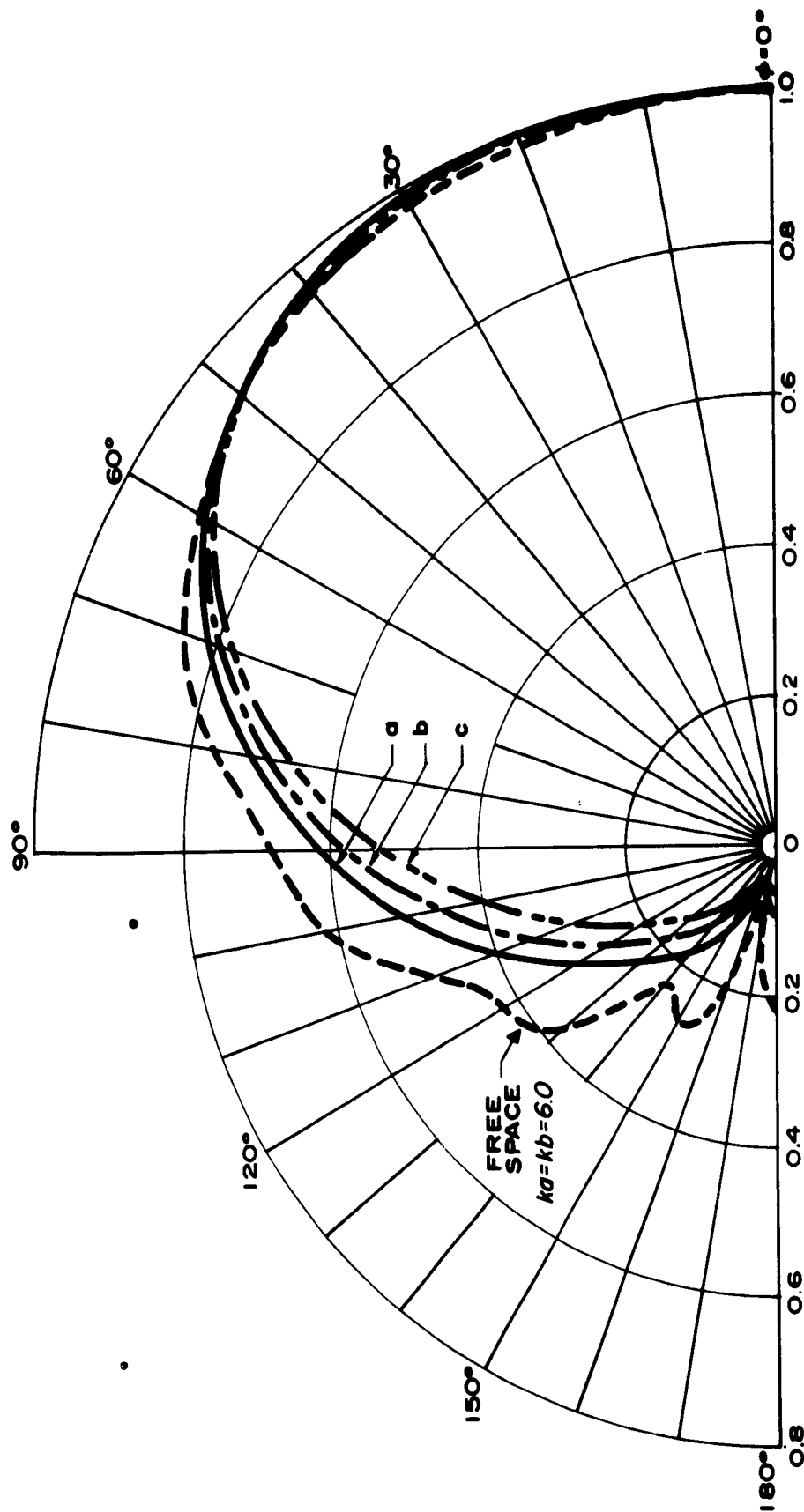
Fig. 3   Field Patterns For Slotted Cylinder With Inhomogeneous Sheath Above Resonance.

a.	$ka = 5.0$,	$kb = 6.0$,	$kc = 4.0$,	$kc_A = 1.5$,	$H = 0.1111$
b.	$ka = 5.0$,	$kb = 6.0$,	$kc = 4.5$,	$kc_A = 2.5$,	$H = 0.1905$
c.	$ka = 5.0$,	$kb = 6.0$,	$kc = 4.8$,	$kc_A = 3.0$,	$H = 0.2778$

FREE
SPACE
$ka = kb = 6.0$

sheath below plasma resonance. The corresponding radial dependence
of dielectric constant and associated electron density are plotted in Fig. 4.
The free-space pattern of a slotted cylinder without any sheath has been
included for reference. This pattern exhibits ripples at large angles
which may be interpreted as interference among circumferentially
directed waves. When an inhomogeneous sheath is present these ripples
no longer exist, with the exception of a small local maximum at 180 deg.,
a characteristic feature of many types of diffraction patterns. In addition,
the sheath patterns indicate increased power radiated in forward directions,
relative to the free-space pattern, with a correspondingly reduced power
radiated toward the rear. It is evident from a comparison of the three
patterns that greater forward enhancement results from steep sheath
gradients.

Although within the sheath the condition

$$\frac{1}{k \epsilon(\rho)} \frac{d\epsilon(\rho)}{d\rho} << 1 \tag{33}$$

is not satisfied, the resulting field patterns in Fig. 3 appear to be
consistent with a quasi-geometrical ray-optics interpretation. Inasmuch
as the dielectric constant increases with increasing radius, each "ray"
emerging from the slot is refracted continuously in the forward direction,
thus reducing or eliminating the effects of circumferential waves and
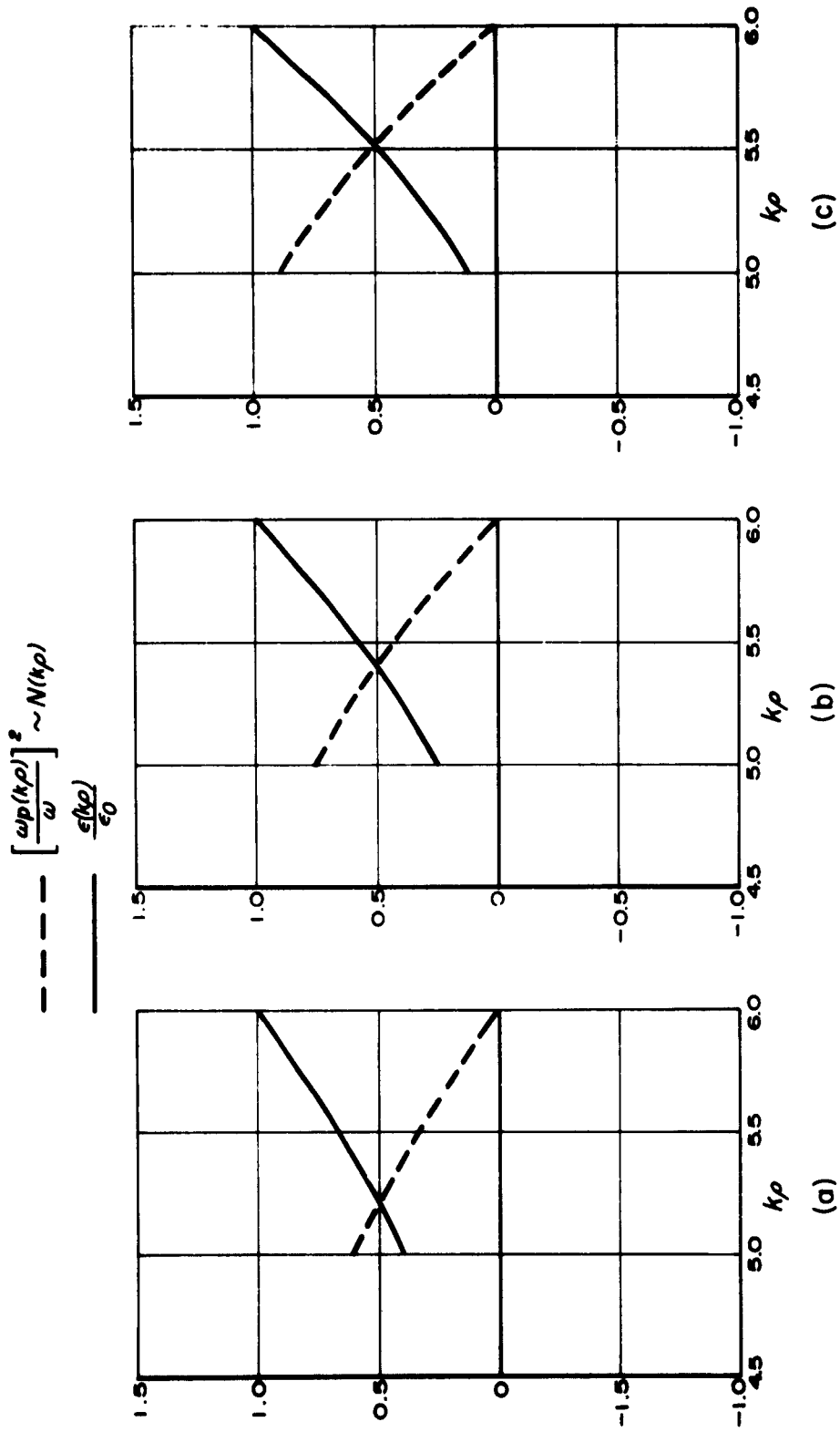producing field patterns enhanced in the forward directions. The steeper

Fig. 4 Radial Dependences Of Dielectric Constant And Electron Density For Inhomogeneous Sheath Above Resonance.

a.	ka = 5.0,	kb = 6.0,	kc = 4.0,	kc_A = 1.5,	H = 0.1111
b.	ka = 5.0,	kb = 6.0,	kc = 4.5,	kc_A = 2.5,	H = 0.1905
c.	ka = 5.0,	kb = 6.0,	kc = 4.8,	kc_A = 3.0,	H = 0.2778

-17-

sheath gradients produce greater bending of the "rays" in the forward direction and, consequently, greater forward enhancement. Although this interpretation appears valid, the steep gradients within the sheaths undoubtedly produce other effects (e.g. scattering) in addition to refraction, all of which are included in Eq. 18, the complete solution of Maxwell's equations.

The field patterns plotted in Figs. 5a, 6a, and 7a have been derived for inhomogeneous sheaths that are partially below plasma resonance. The corresponding dielectric constant variations are plotted in Figs. 5b, 6b, and 7b, respectively. In each case the minimum value of dielectric constant, with the associated maximum electron density, occurs at the inner edge of the sheath, $\rho = a$. It is evident that (1) wide-angle ripples no longer exist, and (2) these patterns are more sharply forward-directed than either the free-space pattern or the patterns considered previously for inhomogeneous sheaths above plasma resonance (cf. Fig. 3).

Propagating waves cannot exist in the region below plasma resonance. Instead the fields are evanescent in nature, decaying strongly along each "ray path". Consequently the strongest "rays" emerging from the cutoff region will have undergone the shortest "ray paths", resulting in a sharply forward-directed pattern. This effect has been previously calculated for homogeneous sheaths below plasma resonance (Ref. 8). The "rays" will undergo additional forward bending upon emerging into the outer region that, although above cutoff, is radially inhomogeneous. Consequently, it is
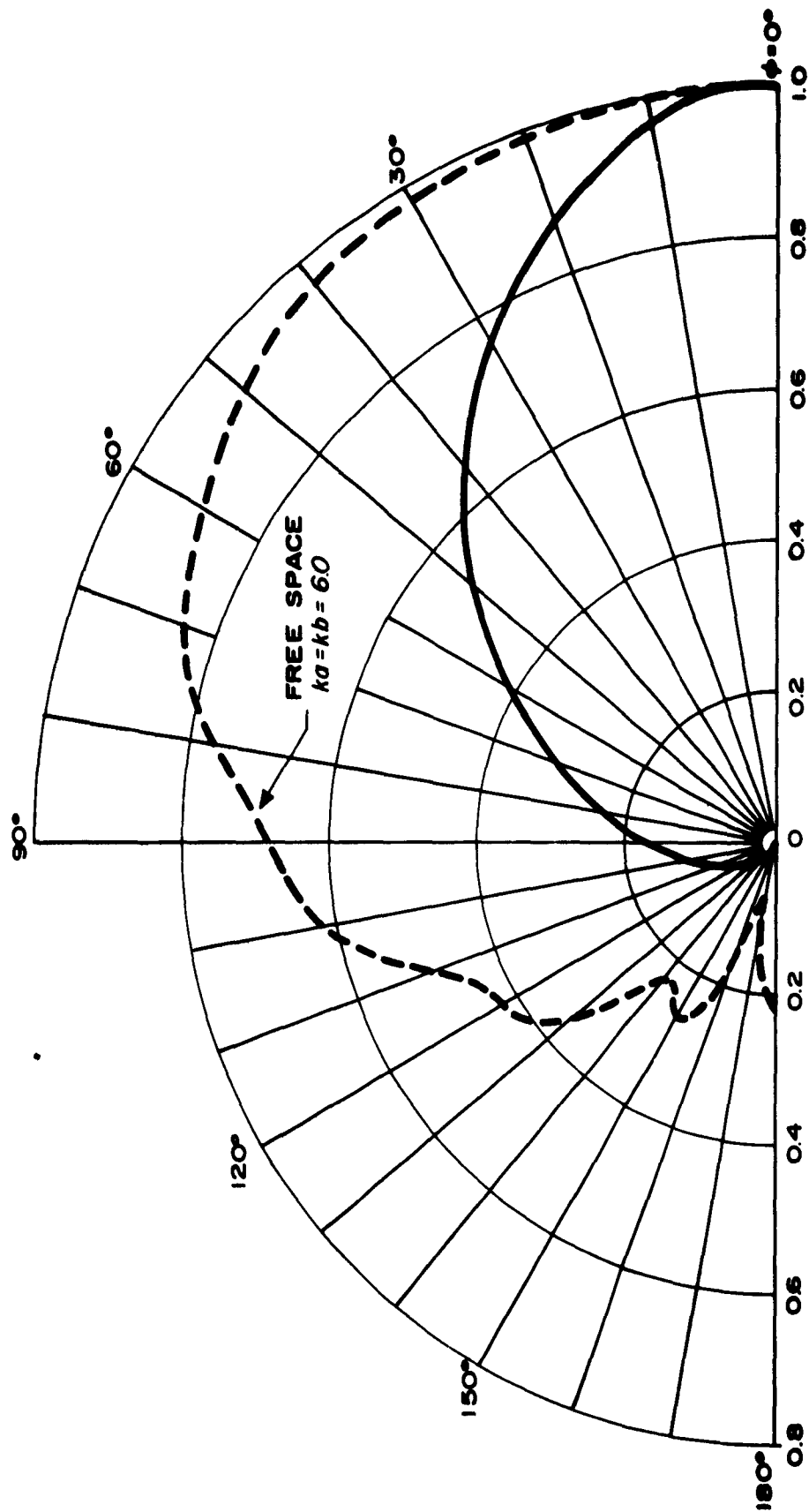
Fig.5a Field Pattern For Slotted Cylinder With Inhomogeneous Sheath Partially Below Resonance.

$ka = 5.0,$ $kb = 6.0,$ $kc = 5.3,$ $kc_A = 4.3,$ $H = 0.8403$

Fig. 5b   Radial Dependence Of Dielectric Constant And Electron
Density For Inhomogeneous Sheath Partially Below
Resonance.

ka = 5.0,   kb = 6.0,   kc = 5.3,   kc$_A$ = 4.3,   H = 0.8403
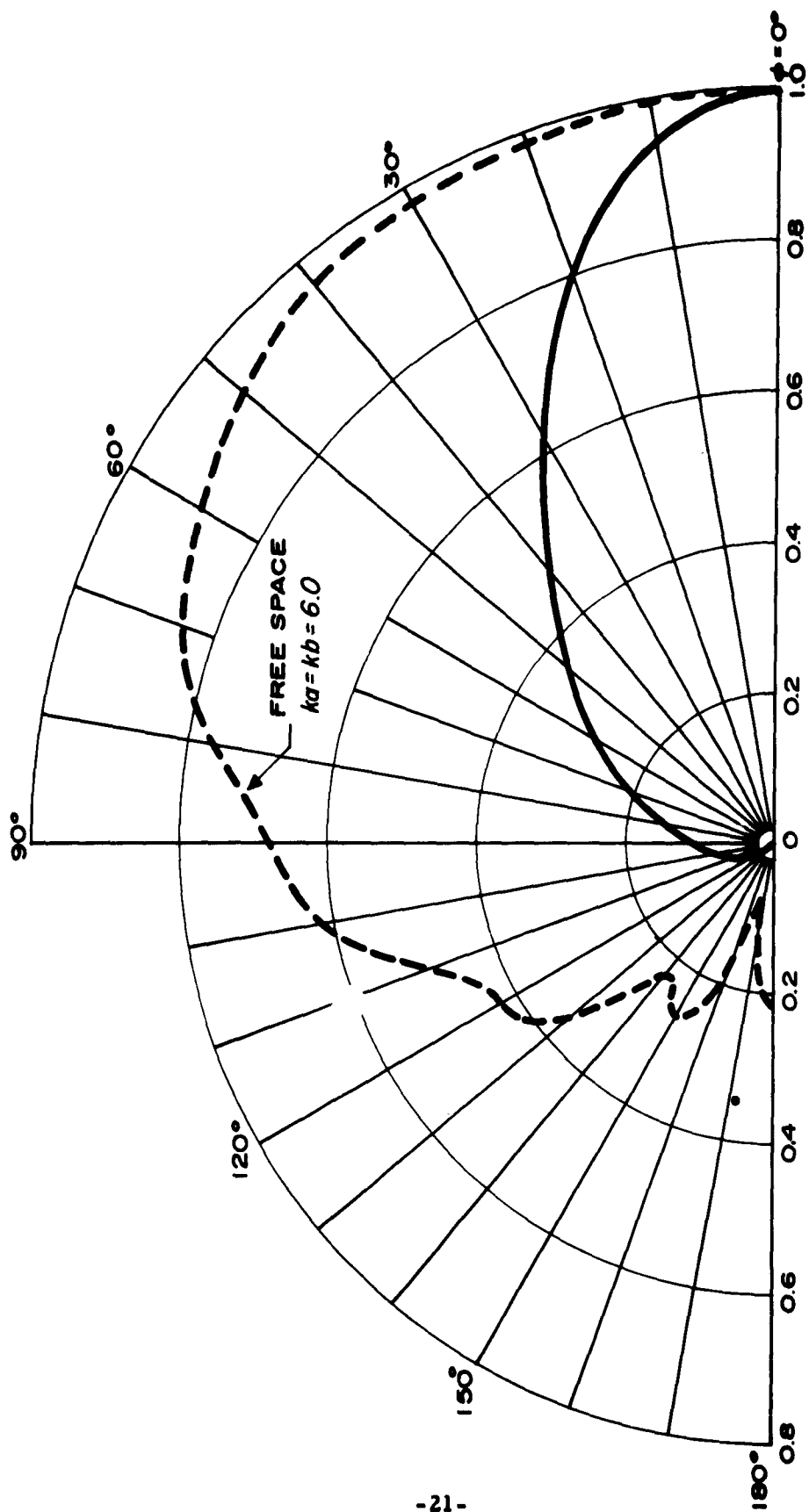
Fig. 6a   Field Pattern For Slotted Cylinder With Inhomogeneous Sheath Partially Below Resonance.

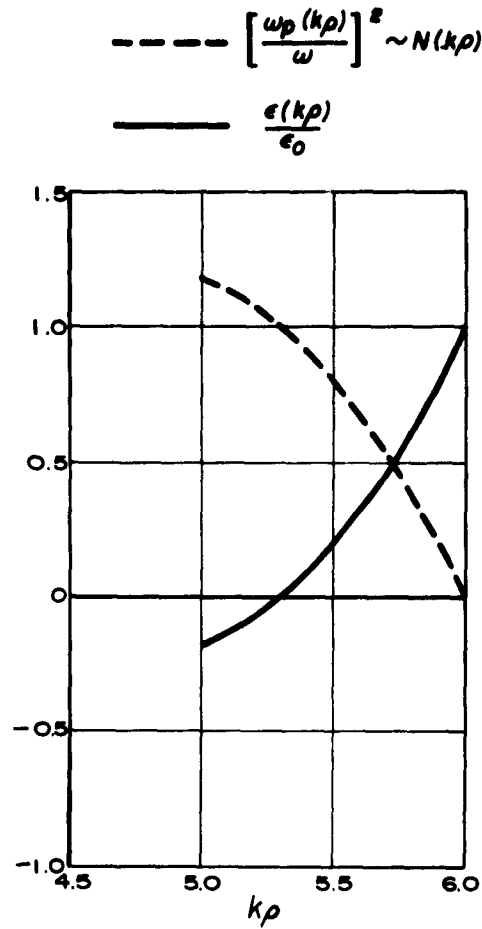ka = 5.0,   kb = 6.0,   kc = 5.5, kc_A = 4.5,   H = 1.3333

Fig. 6b   Radial Dependence Of Dielectric Constant And Electron
Density For Inhomogeneous Sheath Partially Below
Resonance.

ka = 5.0,   kb = 6.0,   kc = 5.5,   kc$_A$ = 4.5,   H = 1.3333

Fig. 7a Field Pattern For Slotted Cylinder With Inhomogeneous Sheath Partially Below Resonance.

ka = 5.0,   kb = 6.0,   kc = 5.8,   kc$_A$ = 4.2,   H = 2.7778

Fig. 7b   Radial Dependence Of Dielectric Constant And Electron
Density For Inhomogeneous Sheath Partially Below
Resonance.
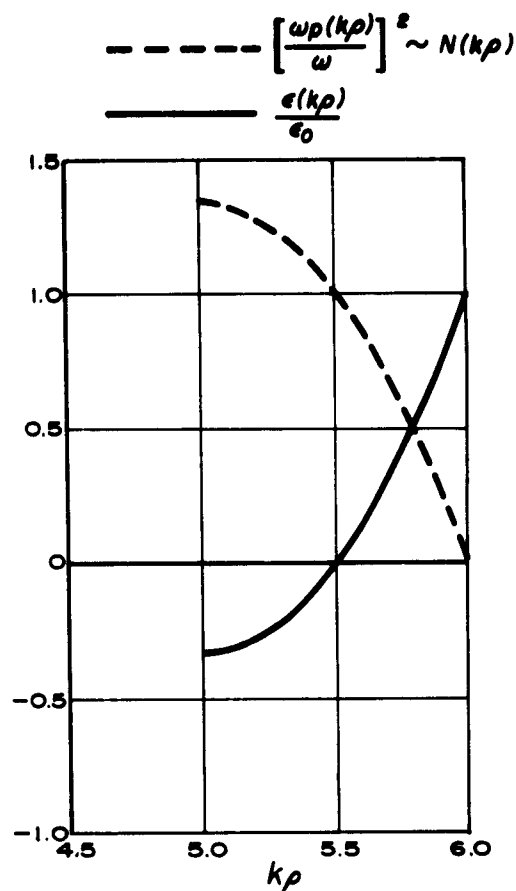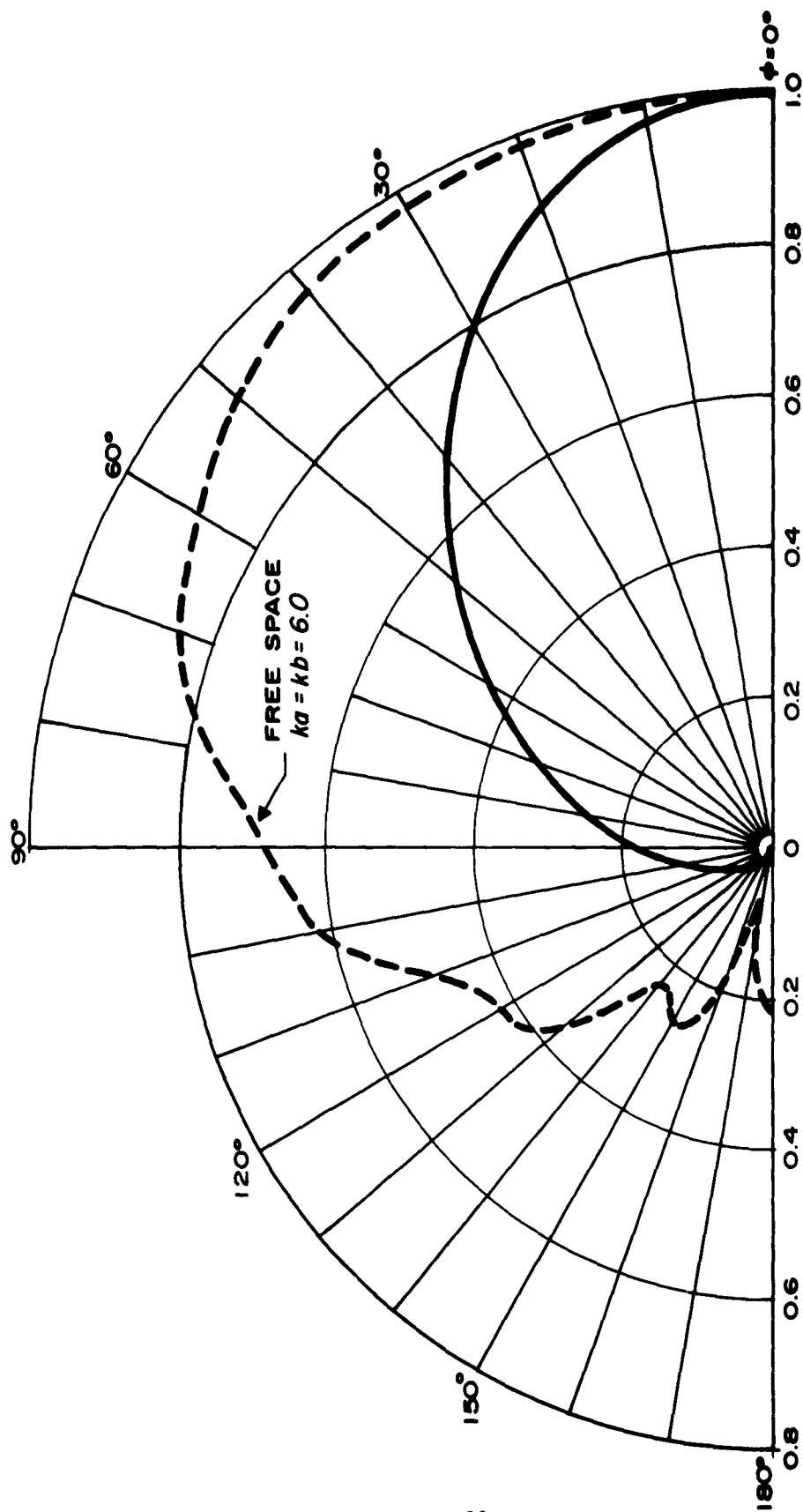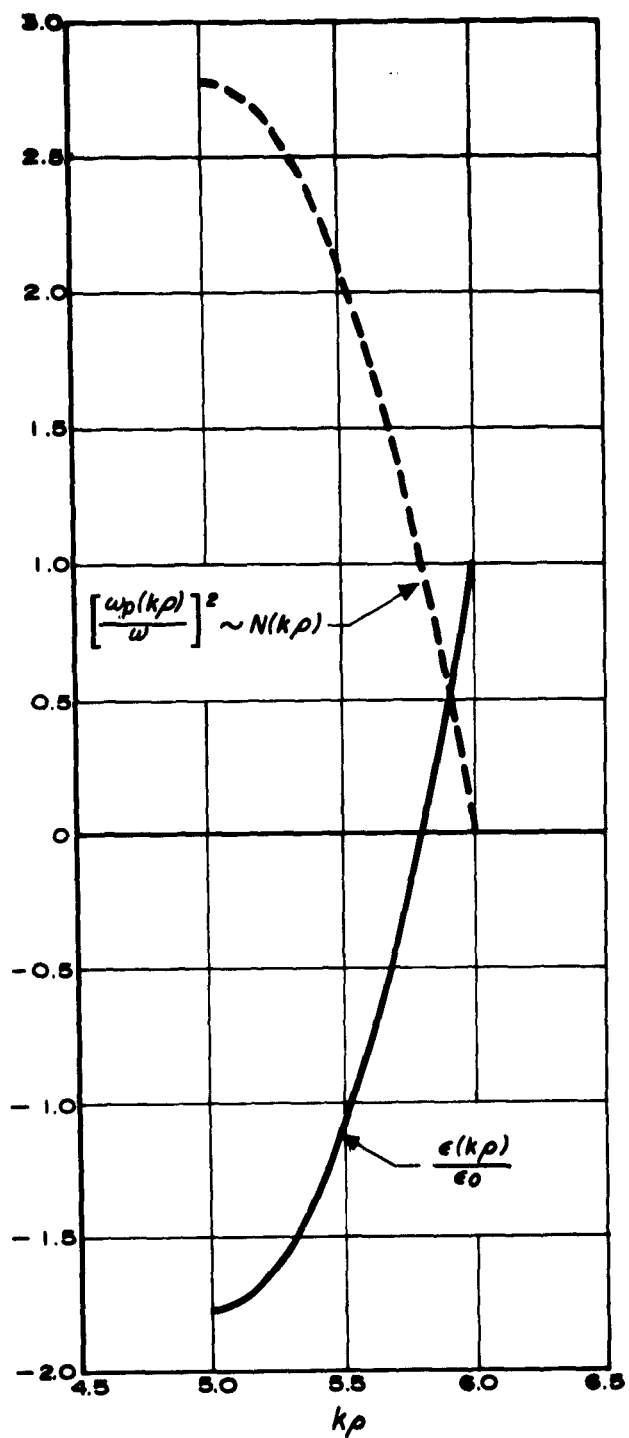
ka = 5.0,   kb = 6.0,   kc = 5.8,   kc$_A$ = 4.2,   H = 2.7778

not unreasonable to assume that both the "diffusion-type" process within the inner region and the "refraction-type" process within the outer will contribute to a relatively sharp maximum in the forward direction. Comparison of Figs. 5-7 with Fig. 3 indicate that processes within the cutoff region may contribute more to the high degree of forward directivity than processes within the outer.

However, the electromagnetic effects taking place within inhomogeneous sheaths of this type are extremely complex. No apparent correlation is evident between pattern features and sheath distributions for the three examples considered in Figs. 5-7. Of the three, Fig. 6a is the most directive, although the corresponding sheath for this pattern is intermediate in both cutoff layer thickness and sheath gradient. Since the dielectric constant becomes zero within the sheaths considered in Figs. 5-7, it is evident from Eq. 33 that the approximations of geometrical ray optics are even less valid than previously. Furthermore, increased gradients may result in more significant scattering effects. A simple interpretation is not readily apparent for sheaths of this type.

The field pattern in Fig. 8a was also derived for an inhomogeneous sheath partially below plasma resonance. However, the minimum value of dielectric constant occurs within the cutoff region at ρ_0 where $\rho_0 > a$, as indicated in Fig. 8b. Again, there is a high degree of directivity in the forward direction. However, there is no significant difference between this pattern and those considered in Figs. 5-7.
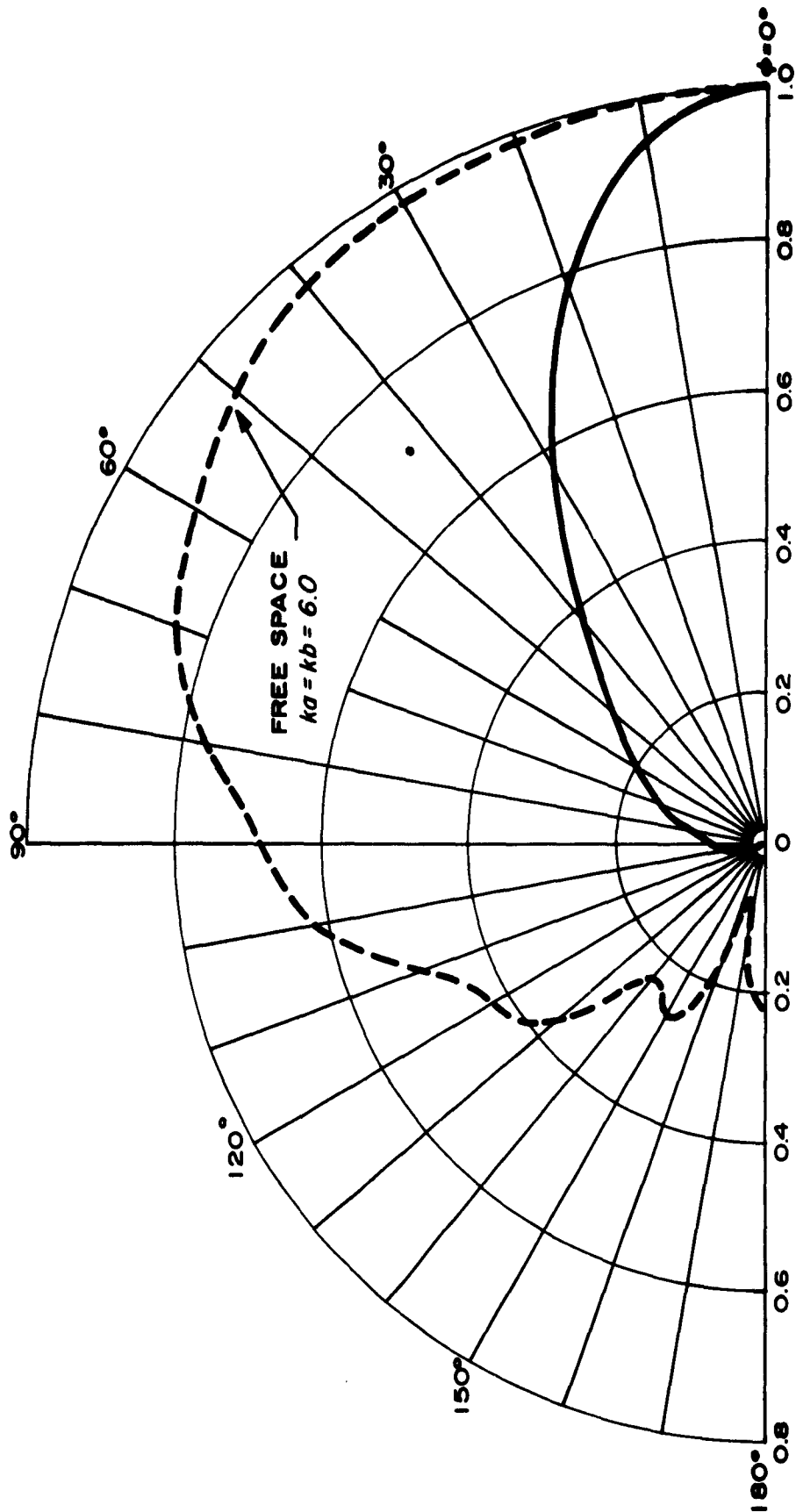
Fig. 8a Field Pattern For Slotted Cylinder With Inhomogeneous Sheath Partially Below Resonance.

ka = 5.0,   kb = 6.0,   kc = 5.5,   kc_A = 4.8,   H = 1.6667
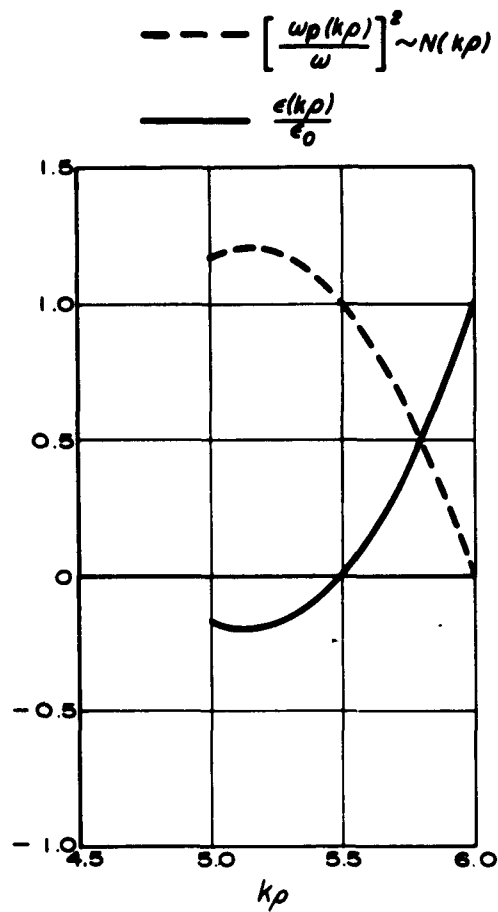
Fig. 8b   Radial Dependence Of Dielectric Constant And Electron
Density For Inhomogeneous Sheath Partially Below
Resonance.

$ka = 5.0$, $kb = 6.0$, $kc = 5.5$, $kc_A = 4.8$, $H = 1.6667$

VII. SERIES CONVERGENCE

The circle of convergence for each of the radial series (Eqs. 25, 26, 27, 28) is defined by $\left| k\rho - kc \right| < (kc - kc_A)$ (Ref. 7). These series converge extremely rapidly if $\left| k\rho - kc \right| < 1$. This condition was satisfied in the computation of Figs. 5-8, i. e., when a portion of the sheath was below plasma resonance. It was found that for $m \leq 34$ (the greatest value of m considered) the 35-term and 99-term series were indistinguishable (to the four significant figures of the computer printout roundoff). As an additional check, the Wronskian relation agreed to within four significant figures. In each case the field patterns were identical for the 35-term and 99-term series.

In cases where $\left| k\rho - kc \right| \geq 1$, a discrepancy in the fourth significant figure was noticed between the 35-term and 99-term series for $m > 12$. This resulted in a slight variation (in the fourth significant figure) in the small values of the field patterns between the 35-term and 99-term results. However, the field patterns were identical for the 60-term and 99-term series, and the Wronskian relations again agreed within the printout roundoff for the 35-term and 99-term series. It was evident that by taking 60 terms or more all series converged to four significant figures for the range of parameters considered. In cases where thicker sheaths or sheaths of larger radius are considered, convergence may be a matter of increased significance.

REFERENCES

1. Rotman, W. and G. Meltz, "Experimental Investigation of the Electromagnetic Effects of Reentry," AFCRL 87, Bedford, Mass., March 1961.

2. Samaddar, S.N., "Wave Propagation in a Cylindrical Wave Guide Containing Inhomogeneous Plasma Involving a Turning Point," Can. J. Phys., Vol.41, No.1, p.113, January 1963.

3. Åström, E., Arkiv Fysik, Vol.19, No.13, p.163, 1961.

4. Ginzburg, V.L., "Propagation of Electromagnetic Waves in Plasma," Gordon and Breach Science Publishers Co., Inc., New York, 1961.

5. Stratton, J.A., "Electromagnetic Theory," McGraw-Hill Book Co., New York, 1941.

6. Hansen, W.W., Phys. Rev., Vol.47, p.139, 1935.

7. Whittaker, E.T. and G.N. Watson, "A Course of Modern Analysis," The Macmillan Company, New York, 1943, Chapter X.

8. Rusch, W.V.T., "Radiation from a Plasma-Clad Axially Slotted Cylinder," J. Research Natl. Bur. Standards, Vol.670, No.2, p.203, March-April 1963.

ACKNOWLEDGMENT

APPENDIX A

DERIVATION OF THE WRONSKIAN RELATIONS

Since both $R_m^{(1)}(k\rho)$ and $R_m^{(2)}(k\rho)$ satisfy Eq. 10, the following pair of equations can be formed:

$$\left\{(k\rho)^2\right\}R_m^{(1)''}(k\rho) + \frac{(k\rho)}{f(k\rho)}\left\{f(k\rho) - (k\rho)\frac{df(k\rho)}{d(k\rho)}\right\}R_m^{(1)'}(k\rho) + \left\{(k\rho)^2 f(k\rho) - m^2\right\}R_m^{(1)}(k\rho) = 0 \tag{A1}$$

$$\left\{(k\rho)^2\right\}R_m^{(2)''}(k\rho) + \frac{(k\rho)}{f(k\rho)}\left\{f(k\rho) - (k\rho)\frac{df(k\rho)}{d(k\rho)}\right\}R_m^{(2)'}(k\rho) + \left\{(k\rho)^2 f(k\rho) - m^2\right\}R_m^{(2)}(k\rho) = 0 \tag{A2}$$

Multiplying (A1) by $R_m^{(2)}(k\rho)$ and (A2) by $R_m^{(1)}(k\rho)$ and subtracting yields:

$$(k\rho)^2\left[R_m^{(1)''}(k\rho)R_m^{(2)}(k\rho) - R_m^{(1)}(k\rho)R_m^{(2)''}(k\rho)\right] + \frac{(k\rho)}{f(k\rho)}\left[f(k\rho) - (k\rho)\frac{df(k\rho)}{d(k\rho)}\right]$$

$$\left[R_m^{(1)'}(k\rho)R_m^{(2)}(k\rho) - R_m^{(1)}(k\rho)R_m^{(2)'}(k\rho)\right] = 0 \tag{A3}$$

This can be rewritten as

$$\frac{d}{d(k\rho)}\,\ell n\left\{R_m^{(1)'}(k\rho)R_m^{(2)}(k\rho) - R_m^{(1)}(k\rho)R_m^{(2)'}(k\rho)\right\} = \frac{d}{d(k\rho)}\,\ell n\left\{\frac{f(k\rho)}{(k\rho)}\right\} \tag{A4}$$

Integrating:

$$R_m^{(1)'}(k\rho)\,R_m^{(2)}(k\rho) - R_m^{(1)}(k\rho)\,R_m^{(2)'}(k\rho) = \frac{Af(k\rho)}{(k\rho)} \tag{A5}$$

The constant of integration, A, can then be evaluated by taking the leading terms of the left-hand side of Eq. A5 as $\rho \to c$. Hence

$$m = 0: \quad A = \frac{(2kc)}{H(kc - kc_A)} \tag{A6}$$

$$m \geq 1: \quad A = \frac{8(kc)^3}{m^2 H(kc - kc_A)} \tag{A7}$$